

ITERATIVE IMAGE RECONSTRUCTION METHODS IN CONE BEAM CT APPLIED TO PHANTOM AND CLINICAL DATA

W. Qiu, M. Soleimani, C. N. Mitchell

Dept. of Electronic and Electrical Engineering, University of Bath, Bath, BA2 7AY, U.K.

T. Marchant, C. J. Moore

The Christie NHS Foundation Trust, Wilmslow Road, Manchester, M20 4BX, U.K.

Keywords: Iterative reconstruction algorithms, Cone beam CT.

Abstract: Cone beam computed tomography (CBCT) enables a volumetric image reconstruction from 2D projection data. In CBCT reconstruction, iterative methods of image reconstruction offer the potential to generate high quality images and would be an advantage especially for sparse data sets. CBCT image reconstruction software has been developed based on Multi-Instrument Data Analysis System (MIDAS) tomography toolbox. In this paper, we present a comparative study of SIRT and ART algorithms, developed in MIDAS platform. The results will be shown using phantom and clinical patient data.

1 INTRODUCTION

Cone beam computed tomography (CBCT) provides a volumetric image reconstruction from tomographic projection data, while in commercial CT system, though many algorithms exist, filtered back projection (FBP) like reconstruction algorithm based on FDK (Feldkamp et al., 1984) is still being used. Recently, iterative reconstruction algorithms are being investigated for clinical application (Wang et al., 2009), as challenges still exist for image reconstruction due to computational time, parameters selection and down sampled data in some practical applications. Iterative algorithms provides an alternative for commercial tomographic image reconstruction methods. In this paper the iterative methods have been studied and results show that they have potential to performed better in various situations, especially when projection data are not fully available (Andersen, 1989). In addition, most of the papers describe the behaviour of iterative algorithms by using phantom data only (Mueller et al., 1999) without applying to clinical patient measurement. In our work, comparison of the CBCT iterative algorithms (ART (Gordon et al., 1970) and SIRT (Gilbert, 1972)) implemented in the Multi-Instrument Data Analysis System (MIDAS) (Mitchell and Spencer, 2003) tomography software are presented by applying to phantom and clinical

data. Convergence rate, edge recovery, computational time and quality of the image are the main criteria for considerations. Results are presented with the image reconstructed from full data sets of CBCT projection data using iterative algorithms (ART and SIRT). They are compared in terms of the criteria mentioned while a FDK image from the same system is used as a reference.

2 THE CBCT SYSTEM AND DATA

In this study, the measured projection data were provided by North Western Medical Physics at The Christie hospital in Manchester. A 'RANDO' anthropomorphic head phantom¹ was scanned to produce 360 X-ray projection images, approximately evenly spaced over an angular range of -100 to +100 degrees. Images were acquired at 100kV, 10mA and 10ms per projection, with total imaging dose of approximately 1.5mGy. Each projection image contains 512x512 pixels of dimension 0.8x0.8mm. Figure 1 shows the imaging system used in this study.

Using the full 360 projection data set a 3D reconstruction of 256x256x256 voxels with resolution 1mm in each direction was produced using iterative

¹The Phantom Laboratory, Salem, NY, USA.

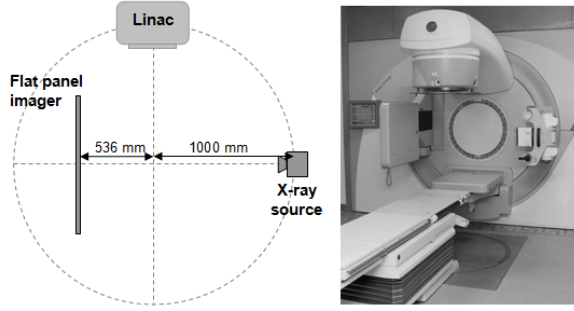


Figure 1: Medical linear accelerator with integrated X-ray cone-beam CT system.

techniques. A 'reference image' was reconstructed using the COBRA cone beam software developers package from EXXIM². This contains an implementation of FDK FBP, which is a useful benchmark for the iterative techniques described in this paper.

3 METHODS

The classic ART algorithm is

$$f_j^{(i+1)} = f_j^{(i)} + \lambda \frac{p_k - \sum_{n=1}^N f_n^{(i)} w_{nk}}{\sum_{n=1}^N w_{nk}^2} w_{jk} \quad (1)$$

where λ is the relaxation parameter, which controls the convergence rate. $f(x, y, z)$ are the image values; j is the index for the voxel of f ; i is the number of iteration; p is the projection data; k is the total number of rays. N is the number of cells; w is the weighting factor and k is the k th image cell intercepted by the n th ray. Including a relaxation parameter can improve the quality of ART reconstructions, but usually at the expense of the speed of convergence. Depending on the application, different strategies are applied for choosing the most appropriate relaxation parameter and other settings. Besides ART, there is another approach of implementation, which is SIRT and defined as

$$f_j^{(i+1)} = f_j^{(i)} + \lambda \frac{\sum_{n=1}^N [w_{jn}(p_k - \sum_{n=1}^N f_n^i w_{nk}) / \sum_{n=1}^N w_{nk}]}{\sum_{n=1}^N w_{nk}} \quad (2)$$

The convergence of the algorithms are used by comparing the measured and calculated projection data, we define residual norm as

$$\|x\| = \sqrt{x_1^2 + x_2^2 + \dots + x_k^2}, \quad \{1 \leq k \leq N\},$$

where x is a vector of the difference between the calculated and measured data. The differences between the iteratively calculated and measured projection data are then used for comparison as defined in Equation 3.

²Exxim Computing Corporation, Pleasanton, CA, USA.

$$E = \|p^{(i)} - p\| \quad (3)$$

In the mean while, a good residual norm result may not always indicate a good reconstructed image, as it considers the reconstruction from the projection data side and one may not expect the projection data differences to be minimised for the best image, since the forward projection does not take into account all physical processes affecting formation of the projection data. Therefore, comparison is made between images. Besides norm differences comparison, image row profiles are used, concentrating the edge area in Equation 4.

$$P = \sum_{a=1}^N f(a, b, c), \quad \{b \in Z, c \in Z \mid 1 \leq b \leq N, 1 \leq c \leq N\} \quad (4)$$

To compare with the reference image, a scaling parameter σ have been used

$$\Delta P = \sigma P_i / P_{ref} \quad (5)$$

4 RESULTS

The new iterative software has been tested using simulated data as well as phantom data. This has also been use for clinical data. Some results are presented here. Figure 2 shows reconstruction of phantom data using ART, SIRT and FDK.

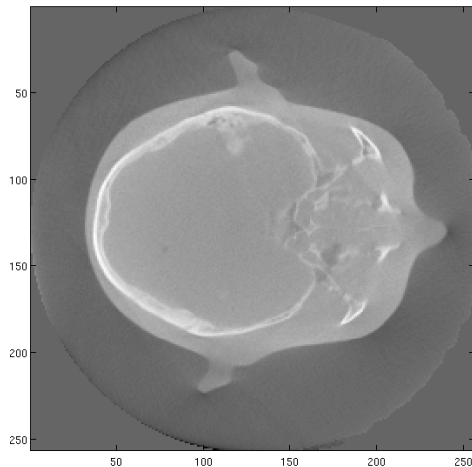
Due to the different behaviour of ART and SIRT, different range of λ are applied. Figure 3 presents the convergence of ART and SIRT, where ART is with λ of 0.0146 while SIRT with λ of 0.45 respectively. It is clearly shown that ART owns a much quicker convergence than SIRT and according to our implementation, it takes about three times more for SIRT to converge the same level of mismatch projection errors as ART.

The computational time for each ART and SIRT iteration is shown in Table 1. It contains not only for full data set, but also down sampled data. The computer used is 64 bit 3.33GHz Linux with ram of 32GB.

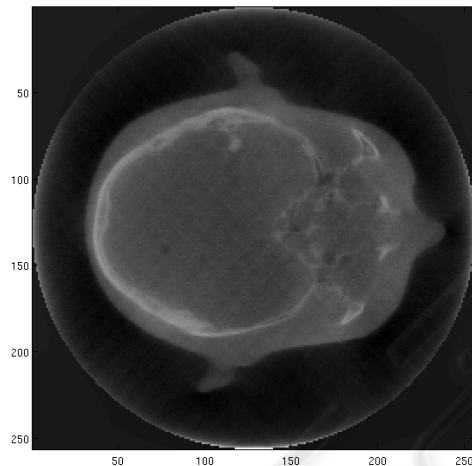
Table 1: Time cost for one ART and SIRT iteration with available data.

	Full data	1/2 data	1/3 data	1/5 data
ART	1600s	800s	540s	320s
SIRT	2200s	1100s	740s	440s

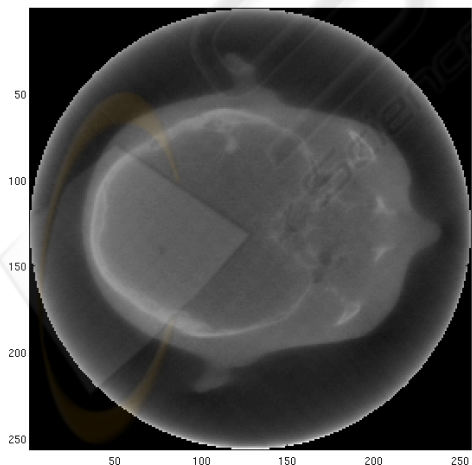
Image row profiles of different iterative algorithms comparing to FDK are then implemented as



(a) FDK reconstruction



(b) ART reconstruction



(c) SIRT reconstruction

Figure 2: Reconstruction with different algorithms using phantom data.

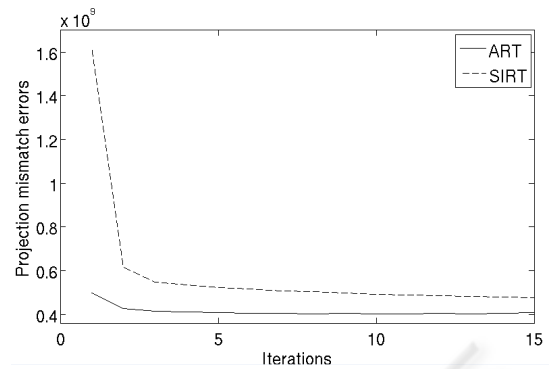


Figure 3: Convergence for ART and SIRT.

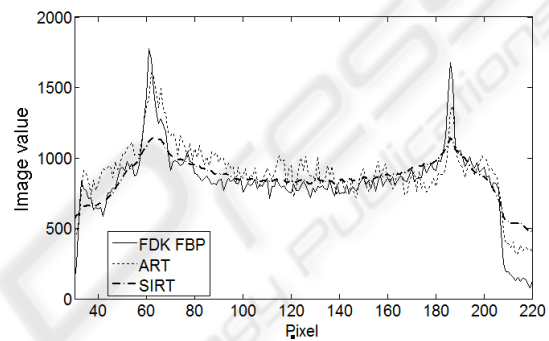
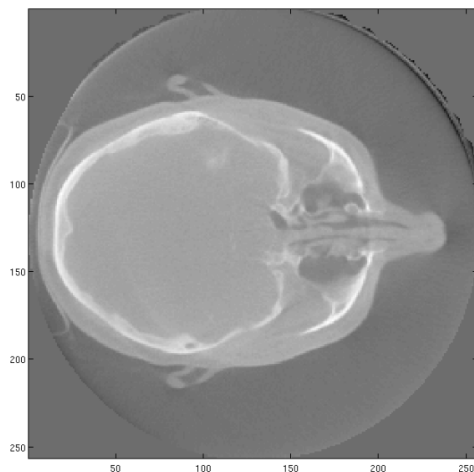


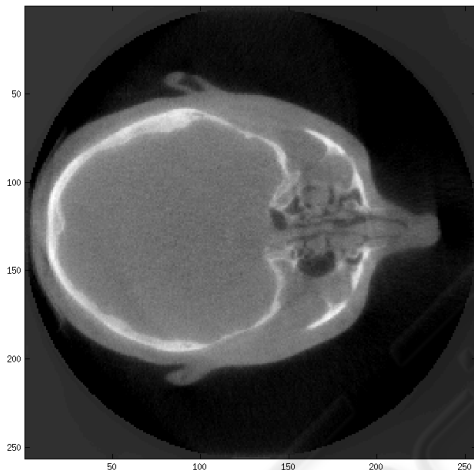
Figure 4: Image profiles for ART, SIRT and FDK FBP at $f(x=128, y, z=128)$.

shown in Figure 4, where ART is with λ of 0.0146 at the 8th iteration using full data set while SIRT with λ of 0.45 at the 40th iteration using full data set respectively. Because ART is sequential method, in which only a single projection is used in each step, whereas SIRT uses all projections in each step simultaneously. SIRT owns a better uniformity than ART and Figure 4 illustrates the expectation. Both the profiles of ART and SIRT are closely fit with the plot of the profiles of FDK. However, compared to SIRT, the plot of ART is more fluctuated, especially from $y = 60 : 180$. The visualised images of ART (with λ of 0.0146, 8th iteration, full data) and SIRT (with λ of 0.45, 40th iteration, full data) are presented in Figure 2(b) and 2(c).

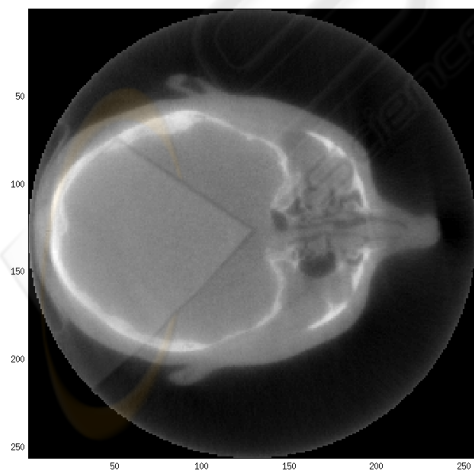
The implementation and phantom results suggest that the ART is more efficient provides suitable results, but by considering the quality of the reconstructed image, SIRT performs better due to the fact that ART is sequential method but SIRT updates the image simultaneously. Figure 5 shows reconstruction of ART and SIRT compared to commercial FDK in clinical patient data.



(a) FDK reconstruction



(b) ART applied to clinical data



(c) SIRT applied to clinical data

Figure 5: Reconstruction with different algorithms using clinical patient data.

5 CONCLUSIONS

Iterative reconstructions using ART and SIRT are investigated and implemented in MIDAS. Convergence, computational time, edge recovery and reconstructed images are considered. The results indicate that ART converge faster than the SIRT while SIRT has a better uniformity. The reconstructed image of ART can be improved by updating simultaneously which is considered as simultaneous algebraic reconstruction technique (SART) (Andersen and Kak, 1984) while in terms of speed, various methods exist such as GPU computing which can potential improve the speed by a factor of 40-100 times.

In our continued effort we are working towards further optimisation of iterative methods as well as their clinical relevance, especially when down sampled data are applied. The MIDAS platform will enable us to develop further innovative approaches. As this work is rapidly progressing and we are hoping to present more results during conference presentation.

REFERENCES

- Andersen, A. H. (1989). Algebraic reconstruction in CT from limited views. *IEEE Transactions on Medical Imaging*, 8(1):50–55.
- Andersen, A. H. and Kak, A. C. (1984). Simultaneous algebraic reconstruction technique (SART): a superior implementation of the ART algorithm. *Ultrasonic imaging*, 6(1):81–94.
- Feldkamp, L. A., Davis, L. C., and Kress, J. W. (1984). Practical cone-beam algorithm. *Journal of the Optical Society of America A*, 1(6):612–619.
- Gilbert, P. (1972). Iterative methods for the three-dimensional reconstruction of an object from projections. *Journal of Theoretical Biology*, 36(1):105–117.
- Gordon, R., Bender, R., and Herman, G. T. (1970). Algebraic reconstruction techniques (ART) for three-dimensional electron microscopy and X-ray photography. *Journal of Theoretical Biology*, 29(3):471–481.
- Mitchell, C. N. and Spencer, P. (2003). A three-dimensional time-dependent algorithm for ionospheric imaging using GPS. *Annals of Geophysics*, 46(4):687–696.
- Mueller, K., Yagel, R., and Wheller, J. J. (1999). Anti-aliased three-dimensional cone-beam reconstruction of low-contrast objects with algebraic methods. *IEEE Transactions on Medical Imaging*, 18(6):519–537.
- Wang, J., Li, T., and Xing, L. (2009). Iterative image reconstruction for CBCT using edge-preserving prior. *Medical Physics*, 36(1):252–260.